

## Bioleaching of a complex nickel–iron concentrate by mesophile bacteria

L.R.G. Santos <sup>a</sup>, A.F. Barbosa <sup>a</sup>, A.D. Souza <sup>b</sup>, V.A. Leão <sup>a,\*</sup>

<sup>a</sup> Universidade Federal de Ouro Preto, Department of Metallurgical and Materials Engineering, Núcleo de Valorização de Materiais Minerais, Praça Tiradentes, 20, Centro, Ouro Preto, MG 35400-000, Brazil

<sup>b</sup> Votorantim Metais, Technologies Development Centre, BR 040, Km. 274, Três Marias, MG 39205-000, Brazil

Received 27 December 2005; accepted 1 March 2006

Available online 25 April 2006

### Abstract

This work investigates the bioleaching of a complex nickel–iron concentrate (pentlandite, pyrrhotite, and minor amounts of chalcopyrite) using acidophile iron-oxidizing bacteria. It aims to improve the understanding of the mechanism of bacterial action on nickel sulphide bioleaching. The effects of the external addition of Fe(II) and the mineralogical assembly on the extraction of nickel are evaluated. A high nickel extraction (around 70%) can be achieved in batch experiments. Moreover, the external addition of iron has not shown any effect on the extraction of the metal, emphasizing the importance of pyrrhotite dissolution in the first step of bioleaching. It was also examined the morphological features of the sulphides as well as the leach residues and reactions products formed during bioleaching. It was noticed that elemental sulphur was produced on pyrrhotite surfaces, which dissolves ahead of pentlandite. A discussion on how galvanic interactions affect the reactivity of sulphide mineral and the formation of bioleaching products is also presented.

© 2006 Elsevier Ltd. All rights reserved.

**Keywords:** Particle morphology; Bioleaching; Sulphide ore

### 1. Introduction

Bioleaching of sulphide minerals is a mature technology with many industrial applications. Refractory gold ores as well as copper and zinc sulphides are some examples of ores amenable to bioleaching (Nemati et al., 1998). It is considered that bioleaching takes place by two different mechanisms: (i) *direct*, where bacteria attached to the mineral surface produce a series of compounds that break up sulphur–metal and sulphur–sulphur bonds. Cysteine seems to play a key role in this mechanism, specially in the case of pyrite biooxidation (Rojas-Chapana and Tributsch, 2000, 2001); (ii) *indirect*, where bacteria oxidize Fe(II) to Fe(III) and utilize electrons in their metabolic processes (Schippers and Sand, 1999). Iron(III), a powerful oxidant, is able to chemically oxidize the majority of sulphide minerals.

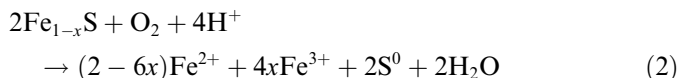
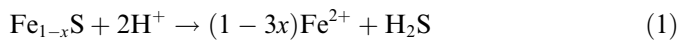
As sulphide minerals have semiconductor properties, galvanic interactions appear when electrical contact among different mineralogical phases occurs. These galvanic effects are important in the aqueous processing of ores and minerals, such as flotation and leaching. Galvanic interactions can substantially increase both leaching rate of and metal recovery from different minerals (Cruz et al., 2005).

During dissolution of a mineral assembly of different sulphides, those minerals that have the highest rest (reduction) potentials behave as cathodes. The oxidant is reduced to its reduced form on their surface. Simultaneously, electrons are removed from the sulphides having the lowest rest potentials (Venkatachalam, 1998). The latter behave as anodic sites where usually sulphide is oxidized to either elemental sulphur or sulphate. Pyrite is an example of a mineral that is usually oxidized directly to sulphate (Schippers and Sand, 1999) while the oxidation of pyrrhotite generates elemental sulphur. Acidophile bacteria such as *Acidithiobacillus ferrooxidans* and *Acidithiobacillus thiooxidans* can oxidize elemental sulphur during bioleaching (Boon, 2001).

\* Corresponding author. Tel./fax: +55 31 3559 1561.

E-mail addresses: [adelson@vmetais.com.br](mailto:adelson@vmetais.com.br) (A.D. Souza), [versiane@demet.em.ufop.br](mailto:versiane@demet.em.ufop.br) (V.A. Leão).

Nickel concentrates produced from sulphides ores usually contain different proportions of iron sulphides (pyrrhotite and pyrrhotite) and nickel (pentlandite, for instance). As pentlandite usually has high rest potentials while pyrrhotite shows lower values, in those ores containing only pyrrhotite and pentlandite, the rest potential indicates that the former dissolves faster than the latter given a certain set of conditions (Lu et al., 2000). The proposed reactions for pyrrhotite dissolution are as follows (Mason and Rice, 2002):



Eqs. (1) and (2) show that as the pyrrhotite dissolves, Fe(II) is being released, providing iron for bacterial growth and further mineral oxidation. Ferrous iron dissolved during pyrrhotite leaching can be further oxidized by *A. ferroxidans* and *L. ferroxidans* to maintain an  $E_h$  high enough to sustain the leaching process (Druschel et al., 2004).

Very few works have focused on pentlandite bioleaching and the reaction products formed. Therefore, the main aim of the present work is to study the effects of external addition of  $\text{Fe}^{2+}$  and mineral association on the bioleaching of a complex nickel sulphide concentrate. Also performed is a characterization of the leach residues aiming to improve the understanding of the effects of galvanic interactions on the reactivity of sulphide mineral and the formation of bioleaching products.

## 2. Materials and methods

### 2.1. Ore and concentrate samples

A complex sulphide concentrate sample, kindly provided by Mineração Serra da Fortaleza (Grupo Votorantim, Brazil) was studied. The sample had a particle size of 80% – 47  $\mu\text{m}$  and was used as received. Specific surface area of the solid particles was determined as 2.13  $\text{m}^2/\text{g}$  by nitrogen absorption (BET isotherm) in a NOVA 1000

Table 1  
Chemical composition of the concentrate sample

Ni (%)	Fe (%)	Co (%)	Cu (%)	S (%)	Specific surface area ( $\text{m}^2/\text{g}$ )
5.9	28.1	0.4	0.1	21.2	2.13

device. The chemical analysis of the concentrate is shown in Table 1.

Mineralogical characterization was first performed by optical microscopy using a *Leica* phase contrast microscopy. For this analysis the samples were mounted in epoxy resin and then polished to a flat, mirrored surface. Polished sections were viewed under plane polarised light at magnifications of 200 $\times$ , 300 $\times$  and 400 $\times$ .

X-ray diffraction (XRD) and energy dispersive X-ray spectroscopy (EDS) analyses of the concentrate revealed pentlandite, pyrrhotite, and chalcopyrite as the main sulphide phases. Moreover, magnetite, quartz, and silicates were also observed (actinolite, willemseite; actinolite and antigorite). The main minerals, pentlandite and pyrrhotite, were not completely liberated exhibiting very fine and intimately associated grains (Fig. 1). Based on the chemical analysis, it was estimated to contain roughly 40% pyrrhotite, 17% pentlandite and 0.3% chalcopyrite in the concentrate.

### 2.2. Microorganisms and nutrient solution

The microorganisms were isolated from a Brazilian zinc sulphide mine and previous biooxidation studies have shown that the bacteria are capable to oxidize ferrous iron and sulphur (Daman et al., 2002; Pina et al., 2005). Prior the bioleaching experiment, the bacteria were adapted to the concentrate for at least 12 weeks. The microorganisms were cultured in 250 mL shake flasks using an orbital incubator with a stirring speed of 200  $\text{min}^{-1}$  at a constant temperature (34  $^\circ\text{C}$ ). A sterilised medium was used for bacteria growth, composed of 0.2 g/L  $(\text{NH}_4)_2\text{SO}_4$ ; 0.4 g/L  $\text{MgSO}_4 \cdot 7\text{H}_2\text{O}$  and 0.1 g/L de  $\text{K}_2\text{HPO}_4$  (*Synth*). Samples of concentrate were used as the energy source. The cultures

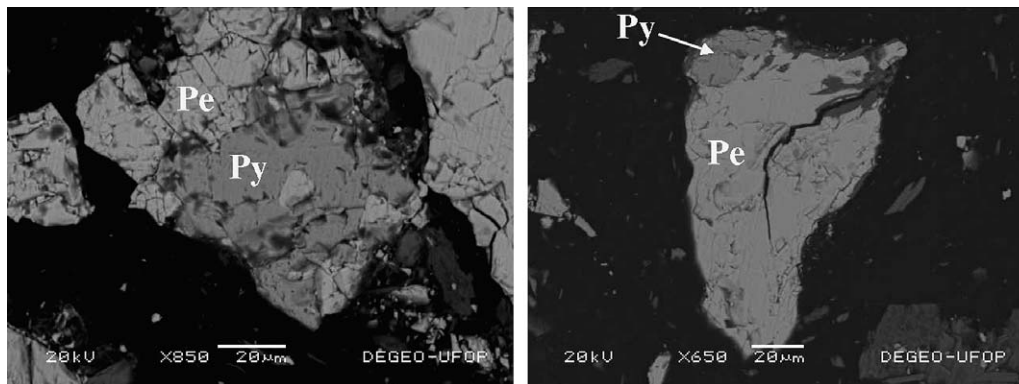


Fig. 1. Scanning electron microscope images of the sulphides present on the nickel concentrate showing association between pentlandite and pyrrhotite. Pe: pentlandite; Py: pyrrhotite.

were prepared by inoculating bacteria previously cultivated at 5% (w/v) pulp density (pentlandite concentrate).

2.3. Bioleaching experiments

Salt nutrient solution (50 mL) adjusted to the required pH was transferred to 250 mL erlenmeyers and the amount required of Fe(II) was added as a solution containing 50 g/L

Fe(II) (as  $\text{FeSO}_4 \cdot 7\text{H}_2\text{O}$ ). Then 5 g of the concentrate (corresponding to 5% (w/v) pulp density) was added. The flasks were then inoculated with a 10 mL aliquot of the selected culture containing at least  $10^8$  bact/mL and distilled water was added to reach a final slurry volume of 100 mL. An orbital shaker placed in a temperature-controlled room (34 °C) provided mixing. Each flask was sampled on a daily basis by removing a 2-mL aliquot of the leach solution, which was then used for elemental analysis (Ni and Fe) by atomic absorption spectrometry (AAS). The pH was adjusted by using 1 mol/L sulphuric acid or 6 mol/L sodium hydroxide. Evaporation losses were compensated by the addition of distilled water. Sterile controls were also run in the presence of a thymol solution as bactericide.

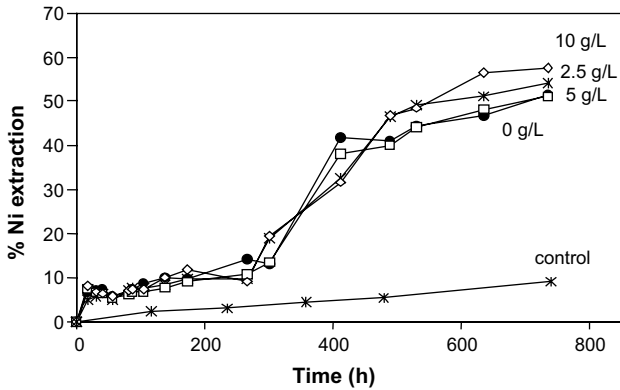


Fig. 2. Effect of Fe(II) addition on nickel extraction from the concentrate by a mesophile iron-oxidizing culture (5% w/v, pH 1.8, 34 °C).

Table 2

Open circuit potential of selected sulphides (McIntosh and Groat, 1997)

Mineral	Open circuit potential (SHE, mV)
Galena (PbS)	300
Chalcocite ( $\text{Cu}_2\text{S}$ )	350
Calcocopyrite ( $\text{CuFeS}_2$ )	400
Pyrrhotite ( $\text{Fe}_{1-x}\text{S}$ )	450
Pentlandite ( $(\text{Fe}, \text{Ni})_8\text{S}_9$ )	550
Pyrite ( $\text{FeS}_2$ )	550–600

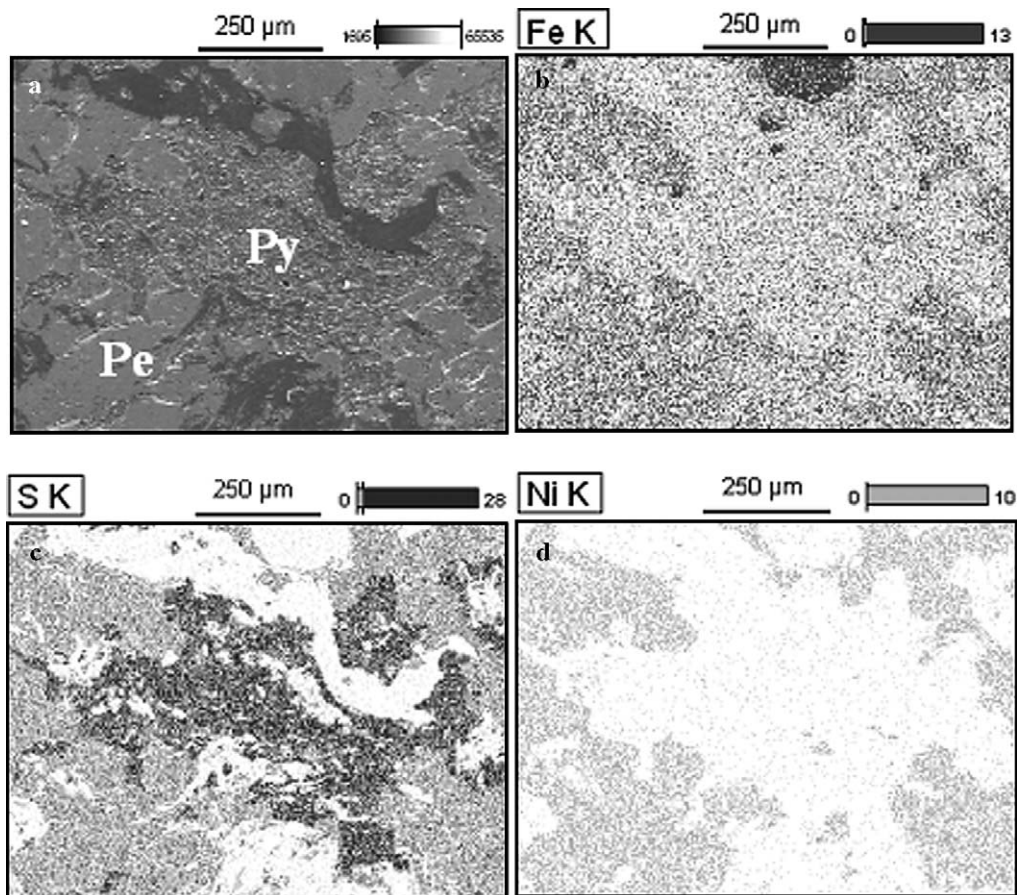


Fig. 3. SEM images of a massive nickel sulphide ore (a) showing the association between pentlandite and pyrrhotite. X-ray energy dispersive spectra of (a) iron; (b) sulphur; (c) nickel of the sample surface. 0 g/L Fe(II) added, pH 1.8, 34 °C. Leaching time: 178 h.



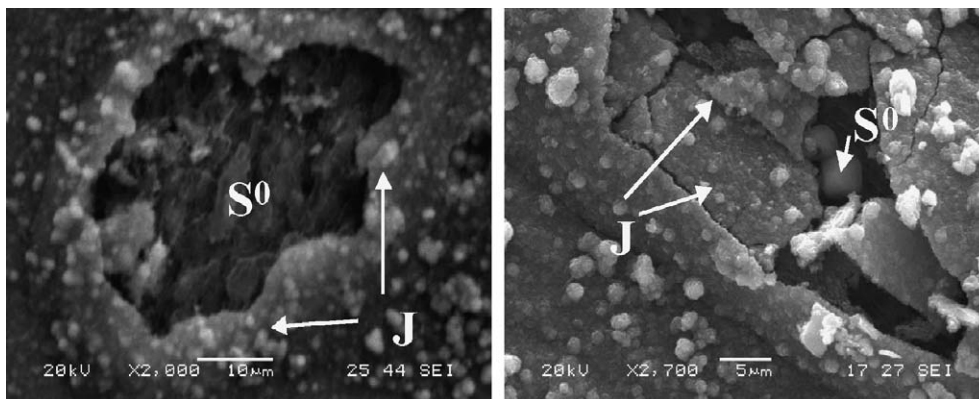


Fig. 4. SEM–EDS images of surface reaction products formed during nickel ore bioleaching in the presence of externally added Fe(II). 2.5 g/L Fe(II) added, pH 1.8, 34 °C. Leaching time: 178 h. J: jarosite.

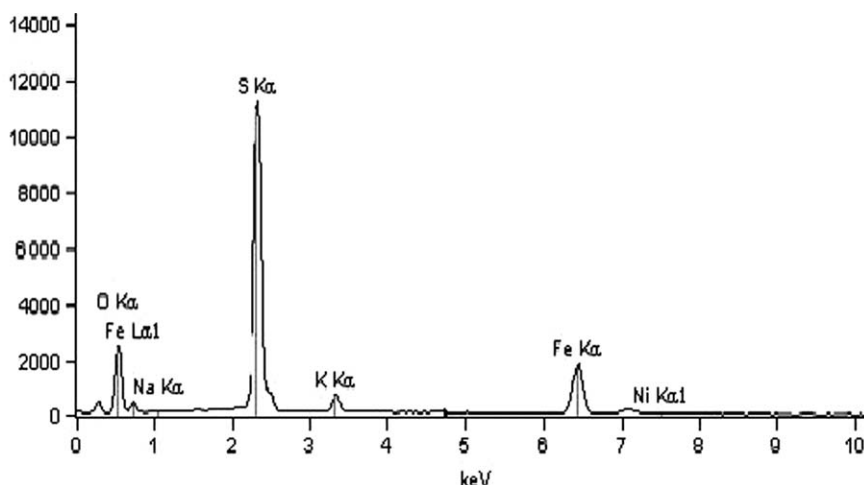


Fig. 5. EDS patterns of the jarosite layer depicted in Fig. 4. Weight concentration: O: 52.42%; Na: 0.49%; S: 28.87%; K: 2.02%; Fe: 15.90%; Ni: 0.21%.

Also assessed was the bioleaching of large pieces (20 × 10 mm) of mixed sulphide (from the same ore deposit that produced the concentrate) with mineralogy as close as possible to that of the concentrate studied. Prior to bioleaching experiments, the pieces were polished and soaked in 3 mol/L hydrochloric acid solution and rinsed with distilled water to remove any oxidation product formed by natural oxidation of the sample. The pH (*Hanna HI931400*) was controlled and the redox potential (*Digimed*) (vs. an Ag/AgCl electrode) recorded.

2.4. Elemental analysis

Concentrate samples were dissolved by treating 0.25 g in 20 mL aqua regia (HNO<sub>3</sub>:HCl 1:3). The resulting solutions were then filtered and diluted to 1000 mL with distilled water prior to analysis. Aqueous metal concentrations (Ni, Co, Cu and total iron) were determined by AAS using a *Perkin–Elmer Analyst 100* device. Sulphur in the concentrate was analysed by direct combustion with infrared detection using *CS244-LECCO* equipment.

2.5. Scanning electron microscopy

The morphological features of the ore, concentrate and leach residues as well as reactions products formed during bioleaching were studied by SEM–EDS. The particles

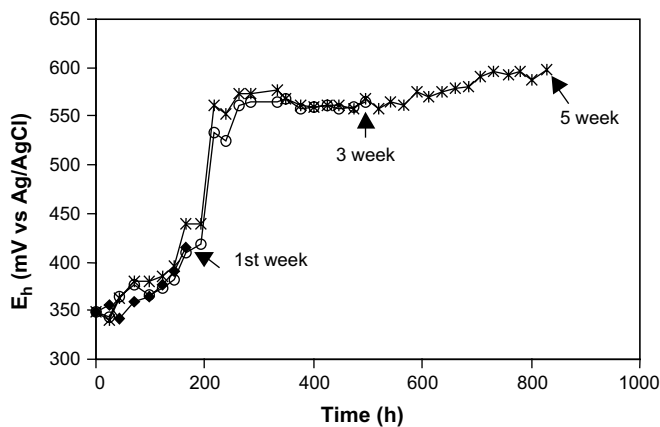


Fig. 6. *E<sub>h</sub>* evolution for three different bioleaching experiments carried out at the same conditions but finished after progressive leaching times. 5.0 g/L Fe(II) added, pH 1.8, 34 °C.

investigated were filtrated and observed as powder or mounted in epoxy resin and then polished to a flat, mirrored surface. Samples were carbon coated and then examined with a JEOL JSM 501 SEM microscope afterwards. Energy dispersive X-ray spectroscopy (EDS) analysis was used for elemental analysis.

### 3. Results and discussion

#### 3.1. Concentrate bioleaching in the presence of externally added Fe(II)

The effect of the presence of Fe(II) (added as FeSO<sub>4</sub>) in the bioleaching of the nickel concentrate is shown in Fig. 2.

From Fig. 2, it can be seen that an external source of Fe(II) is not required for leaching to occur; i.e., nickel extraction is not affected by the amount of Fe(II) added to the reacting system. Similarly,  $E_h$  was not affected by the Fe(II) added either (data not shown). The results suggest that iron dissolution from the concentrate was sufficient to maintain a high potential (Deveci et al., 2004) and sustain nickel dissolution, which is consistent with the mineralogical composition of the concentrate.

Pyrrhotite can be quickly and readily dissolved in acidic solutions liberating Fe(II) and producing H<sub>2</sub>S as depicted in Eq. (1) (Mason and Rice, 2002). As the amount of pyrrhotite can be estimated as around 40% in the concentrate, it is a source of aqueous Fe(II) and therefore provides

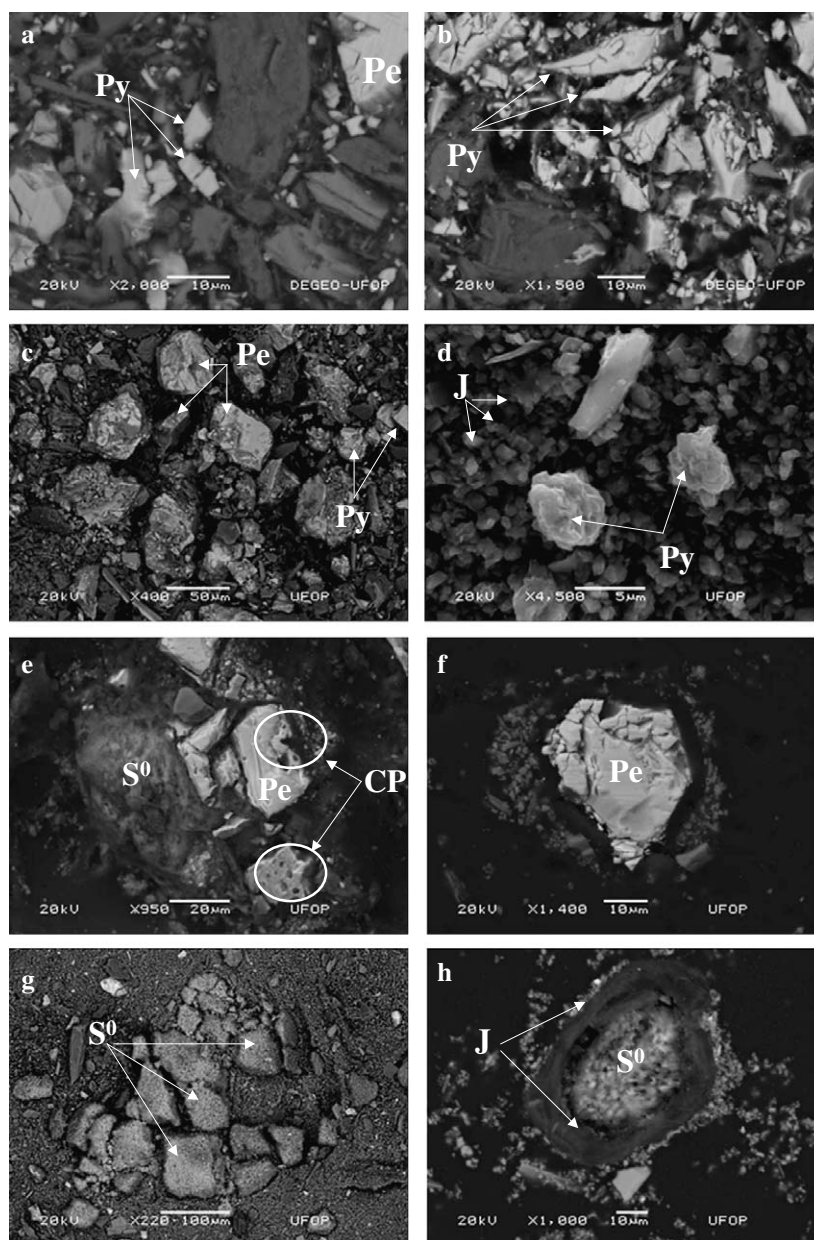


Fig. 7. SEM images of bioleaching residues produced in three different experiments carried out at the same conditions but finished after different leaching times. (a) and (b) concentrate; (c) and (d), after 1 week bioleaching; (e) and (f), after 3 weeks bioleaching; (g) and (h) after 5 weeks bioleaching. Py: pyrrhotite, Pe: pentlandite; J: jarosite; CP: corrosion pit. Experimental conditions 5.0 g/L Fe(II) added, pH 1.8, 34 °C.

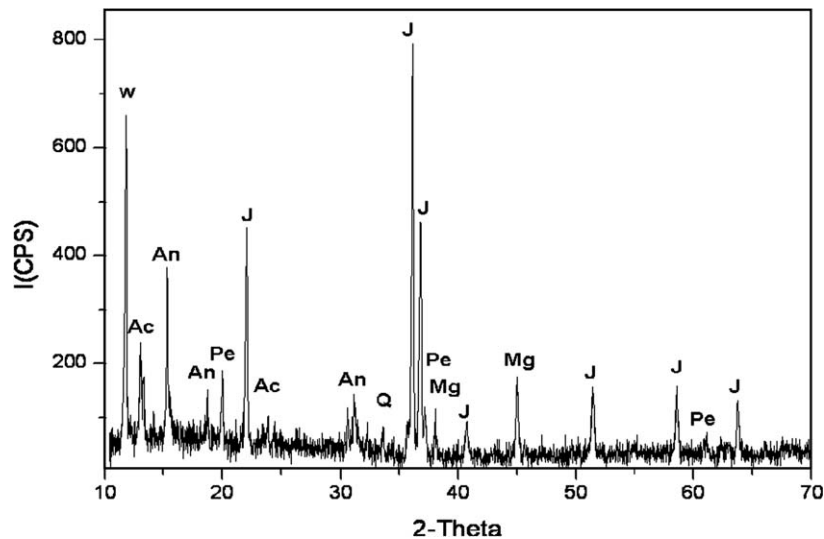


Fig. 8. X-ray diffraction patterns of the leach residue after 35 days of concentrate bioleaching. W: willemseite; J: jarosite; A: actinolite; An: antigorite, M: magnetite; P: pentlandite; Q: quartz.

enough substrate for bacterial growth. In the control test nickel extraction was slow and appeared to be limited by the slow chemical oxidation of iron(II).

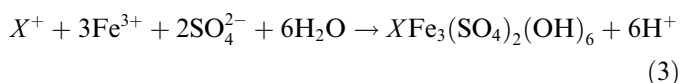
### 3.2. Galvanic effects on the nickel ore

Mineralogical studies have showed the intergrowth of different minerals on the concentrate studied in the present work (Fig. 1) especially pentlandite and pyrrhotite, the main mineralogical constituents. Thus, galvanic interactions may take place during leaching (Cruz et al., 2005). Table 2 presents values of open circuit potentials for different minerals as discussed by McIntosh and Groat (1997). Pentlandite has a higher rest potential than pyrrhotite. Therefore it is expected that during leaching in those conditions where there is an electronic contact between both minerals, pyrrhotite will dissolve anodically and pentlandite will remain inert, i.e., galvanically protected (Cruz et al., 2005).

Experiments were also carried out with a massive sample obtained from the ore that produced the concentrate so that the study of possible galvanic interactions that affect the leaching features of the concentrate is facilitated. This sample was bioleached in the absence of externally added Fe(II) following the procedure applied to the concentrate. As a result, all iron in solution was provided by the dissolution of the ore. Fig. 3a is a SEM image of this massive sample after 178 h of bioleaching showing the association between pentlandite and pyrrhotite. Fig. 3b–d display the X-ray energy dispersive spectra of iron (Fig. 3b), sulphur (Fig. 3c) and nickel (Fig. 3d) for the same region depicted in Fig. 3a. As expected, iron and sulphur predominate throughout the sample while nickel is shown in the regions where pentlandite is the main phase. The regions with the lowest iron content are associated with the dissolution of pyrrhotite while the strongest sulphur concentration is

characterized as elemental sulphur, a reaction product of pyrrhotite dissolution (Thomas et al., 1998). Pentlandite seems less attacked than pyrrhotite. Hence it can be suggested that pyrrhotite is dissolved faster than pentlandite, i.e., the latter is being galvanically protected in the initial steps of bioleaching.

Experiments with iron(II) addition were also carried out. Similar effects could only be inferred however since a probable jarosite layer was formed on the sample surface (specially in pyrrhotite regions) and made the surface analysis more difficult. These features are presented in Fig. 4. Fig. 5 shows the EDS spectrum of the jarosite layer formed on the massive sample surface. Nevertheless, the formation of elemental sulphur in anodic areas is easily seen even below the jarosite layer. At these anodic areas, pyrrhotite dissolution makes iron available to be oxidised by the bacteria. The ferric ions in the presence of sulphate anions and a cation ( $K^+$  for instance) precipitates as jarosite (Toro et al., 1988).



Applying electrochemical techniques, Fowler and Crundwell (1999) showed the importance of bacteria as a catalyst of sulphur oxidation during ZnS bioleaching. In the present work the bacteria did not oxidize all the elemental sulphur formed during leaching since the latter was always observed as a reaction product. Oxidation of pentlandite and pyrrhotite as well as chalcopyrite produced some elemental sulphur (Kuklinskii et al., 2001; Sand et al., 2001; Lu et al., 2002). Due to galvanic interactions elemental sulphur was observed basically on pyrrhotite surfaces while pentlandite shows a less intense attack probably due to galvanic interactions in the sample (Fig. 3). As the bacteria were not able to remove the elemental sulphur, the latter

can act as a barrier to the diffusion of oxidation products away from the solid surface. Hansford and Vargas (2001) stated that the oxidation of elemental sulphur only takes place appreciably in the absence of Fe(II) ions. As iron was dissolved from the concentrate during pyrrhotite leaching, ferrous iron was always available as substrate for bacterial growth. It must also be stressed that pyrrhotite has a lower open circuit potential than pentlandite (Table 2). Consequently, as the potential of the system rises during bioleaching, the driving force for pyrrhotite dissolution becomes larger than that for pentlandite. This behaviour will affect the concentrate dissolution, since considerable pyrrhotite dissolution before pentlandite oxidation is required. Nevertheless actual kinetics information can only be obtained by mixed potentials studies specially in the case of reactive sulphides such as pyrrhotite (Nicol and Lazaro, 2002).

### 3.3. Characterization of the bioleach residue

Based on the previous studies carried out with the ore sample, the analysis of the reaction products was also undertaken on the concentrate after bioleaching. This was accomplished by a SEM–EDS analysis performed on the solid residue of three bioleaching experiments stopped at different solution potentials: 430 mV; 550 mV and 580 mV. Fig. 6 shows that the potential presents basically the same pattern in the three experiments regardless of leaching time, highlighting the good reproducibility of the experimental set up. This feature thus enables the comparison of the reaction products formed at different experiments.

The SEM–EDS analysis of the leaching residue was presented in Fig. 7. Fig. 7a and b shows images of the concentrate before bioleaching. For the experiment ceased at the end of the first week, X-ray and MEV–EDS showed pyrrhotite in the residue (Fig. 7c and d) as a minor phase compared to pentlandite. Interestingly, the remaining pyrrhotite particles as well as the pentlandite grains have morphologies similar to that of the concentrate. The selective dissolution of the finer particles is likely to have taken place as observed in experiments with partial sulphide bioleaching (Pina et al., 2005).

After 3 weeks of bioleaching, the sample was experiencing an  $E_h$  of 550 mV at about 200 h. In this condition it was noticed that pyrrhotite could no longer be observed by either X-ray diffraction or MEV–EDS even though it might be covered by elemental sulphur. This observation was suggested by iron, sulphur and nickel mapping of the region presented in the Fig. 8e (data not shown). Furthermore Fig. 7e and f show pentlandite particles with different morphologies. In Fig. 7e corrosion pits can easily be seen but not in Fig. 7f, which suggests that galvanic interactions may account for the non-dissolution of the pentlandite grain depicted in Fig. 7f. After 35 days, sulphur was seen throughout the sample sometimes near a jarosite layer (Fig. 8) as presented in Fig. 7g and h.

Finally nickel and iron concentrations during the three different bioleaching runs were recorded (Fig. 9). It can be seen that iron concentration increases up to 360 h, after which it starts to precipitate as jarosite or natrojarosite although this behaviour can not be seen in the experiment finished in the first week as expected. Meanwhile, aqueous nickel concentration shows a steady increase that is in agreement with both X-ray diffraction and MEV–EDS observations that suggest that pyrrhotite is the first mineral to leach.

The scenario for a feasible industrial application of bioleaching to nickel sulphide concentrates could involve operation in continuous stirred reactors. This process would be carried out without the necessity of iron addition since the fast pyrrhotite dissolution would provide enough Fe(II) for bacterial growth. Moreover as pentlandite has a large oxidation potential it would be necessary to have high

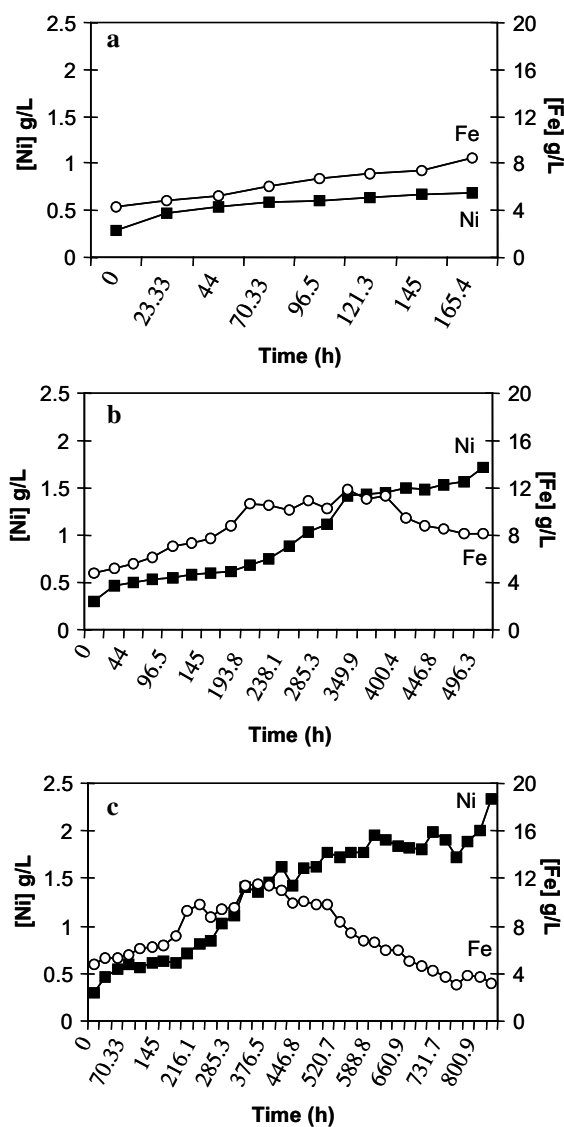


Fig. 9. Nickel and iron profiles during bioleaching of a nickel concentrate. (a) experiment finished after 1 week (b), 3 weeks, (c) 5 weeks. The potential of these experiments are presented in Fig. 6.



potentials in the leaching system for its complete dissolution. This would result in large residence times since due to galvanic interactions it would be expected pyrrhotite dissolution in the first part of the process. This is corroborated by the proposed bioNic™ process in which up to 240 h residence time is required for nickel dissolution (Miller et al., 1997). As an alternative it could also consider bioleaching association with a chemical leaching step in which pyrrhotite would be leached in the bioleaching step followed by the chemical leaching of pentlandite. Another possible approach is to study the heap bioleaching of either the ore or the concentrate since the expected large residence times can be a drawback for the successful application of bioleaching to the processing of nickel sulphides in tanks.

#### 4. Conclusions

The results of this study show that the bioleaching of nickel sulphides can be accomplished with mesophile iron-oxidizing bacteria since nickel extractions as high as 70% can be achieved. Iron(II) addition does not affect bacterial leaching as the dissolution of the concentrate provides enough iron to bacterial growth. It was noticed that elemental sulphur was produced over pyrrhotite surfaces, which dissolves ahead of pentlandite, suggesting that pentlandite dissolution occurs only at high potentials.

#### Acknowledgements

The financial support for this work from “FINACIADORA DE ESTUDOS E PROJETOS—FINEP”, “Instituto do Milênio Água e Mineração” and Votorantim Metais is gratefully appreciated. The “Conselho Nacional de Pesquisas—CNPq scholarship to L. R. G. Santos is also acknowledged.

#### References

- Boon, M., 2001. The mechanism of “direct” and “indirect” bacterial oxidation of sulphide minerals. *Hydrometallurgy* 62, 67–70.
- Cruz, R., Luna-Sánchez, R.M., Lapidus, G.T., González, I., Monroy, M., 2005. An experimental strategy to determine galvanic interactions affecting the reactivity of sulfide mineral concentrates. *Hydrometallurgy* 78, 198–208.
- Daman, D., Leão, V.A., Silva, C.A., Gomes, F.J., 2002. Bioxidação de esfalerita brasileira por *Acidithiobacillus* sp. In: Baltar, C.A.M., Oliveira, J.C.S., Barbosa, J.P. (Eds.), XIX Encontro Nacional de Tratamento de Minérios e Metalurgia Extrativa. Recife, Brazil, pp. 76–82 (In Portuguese).
- Deveci, H., Akeil, A., Alp, I., 2004. Bioleaching of complex zinc sulphides using mesophilic and thermophilic bacteria: comparative importance of pH and iron. *Hydrometallurgy* 73, 293–303.
- Druschel, G.K., Baker, B.J., Gihring, T.M., Banfield, J.F., 2004. Acid mine drainage biogeochemistry at Iron Mountain, California. *Geochemical Transactions* 5, 13–31.
- Fowler, T.A., Crundwell, F.K., 1999. Leaching of zinc sulphide by *Thiobacillus ferrooxidans*: bacterial oxidation of the sulphur product layer increases the rate of zinc sulphide dissolution at high concentrations of ferrous iron. *Applied and Environmental Microbiology* 65 (12), 5285–5292.
- Hansford, G.S., Vargas, T., 2001. Chemical and electrochemical basis of bioleaching processes. *Hydrometallurgy* 59, 135–145.
- Kuklinskii, A.V., Mikhlin, Y.L., Pashkov, G.L., Kargin, V.F., Asanov, I.P., 2001. Conditions of the formation of non-equilibrium nonstoichiometric layer on pyrrhotite in acid solutions. *Russian Journal of Electrochemistry* 37, 1269–1276.
- Lu, Z.Y., Jeffrey, M.I., Zhu, Y., Lawson, F., 2000. Studies of pentlandite leaching in mixed oxygenated acidic chloride–sulfate solutions. *Hydrometallurgy* 56, 63–74.
- Lu, Z.Y., Jeffrey, M.I., Lawson, F., 2002. The effect of chloride ions on the dissolution of chalcopyrite in acid solutions. *Hydrometallurgy* 56 (2), 189–202.
- Mason, L.J., Rice, N.M., 2002. The adaptation of *Thiobacillus ferrooxidans* for the treatment of nickel–iron sulphide concentrates. *Minerals Engineering* 15, 795–808.
- McIntosh, J.M., Groat, L.A., 1997. Biological–mineralogical interactions. Mineralogical association of Canada, Short course series, Ottawa.
- Miller, D.M., Dew, D.W., Norton, A.E., Cole, P.M., Benetis, G., 1997. The BioNIC process: description of the process and presentation of pilot plant results. In: Cooper, W.C., Mihaylov, I. (Eds.), Nickel–Cobalt 97 Hydrometallurgy and Refining of Nickel and Cobalt. CIM, pp. 97–110.
- Nemati, M., Harrison, S.T.L., Hansford, G.S., Webb, C., 1998. Biological oxidation of ferrous sulphate by *Thiobacillus ferrooxidans*: a review on the kinetic aspects. *Biochemical Engineering Journal* 1 (1), 171–190.
- Nicol, M.J., Lazaro, I., 2002. The role of  $E_H$  measurements in the interpretation of the kinetics and mechanisms of the oxidation and leaching of sulphide minerals. *Hydrometallurgy* 63, 15–22.
- Pina, P.S., Leão, V.A., Silva, C.A., Souza, A.D., Frenay, J., 2005. Efeito da biolixiviação sobre a cinética de dissolução de um concentrado sulfetado de zinco em soluções ácidas de sulfato férrico. In: XXI Encontro Nacional de Tratamento de Minérios e Metalurgia Extrativa. Natal, Brazil, pp. 1–6 (In Portuguese).
- Rojas-Chapana, J.A., Tributsch, H., 2000. Bio-leaching of pyrite accelerated by cysteine. *Process Biochemistry* 35, 815–824.
- Rojas-Chapana, J.A., Tributsch, H., 2001. Biochemistry of sulfur extraction in bio-corrosion of pyrite by *Thiobacillus ferrooxidans*. *Hydrometallurgy* 59, 291–300.
- Sand, W., Gehrke, T., Gorg Jozsa, P., Schippers, A., 2001. (Bio)chemistry of bacterial leaching—direct vs. indirect bioleaching. *Hydrometallurgy* 59 (02–03), 159–175.
- Schippers, A., Sand, W., 1999. Bacterial leaching of metal sulfides proceeds by two indirect mechanisms via thiosulfate or via polysulfides and sulfur. *Applied and Environmental Microbiology* 65 (1), 319–321.
- Thomas, J., Jones, C.S., Smart, R.W., 1998. The role of surface sulfur species in the inhibition of pyrrhotite dissolution in acid conditions. *Geochimica et Cosmochimica Acta* 62, 1555–1565.
- Toro, R., Paponetti, D., Cantalini, C., 1988. Precipitate formation in the oxidation of ferrous ions in the presence of *Thiobacillus ferrooxidans*. *Hydrometallurgy* 20, 1–9.
- Venkatachalam, S., 1998. *Hydrometallurgy*, first ed. Narosa Publishing house, Nova Delhi, 318pp.